

## **Characteristics of shallow water waves off the central west coast of India before, during and after the onset of the Indian summer monsoon**

M.M.Amrutha<sup>1</sup>, V. Sanil Kumar<sup>1\*</sup>, Sheela Sharma, Jai Singh<sup>1</sup>, R.Gowthaman<sup>1</sup>, R.S.Kankara<sup>2</sup>

<sup>1</sup>Ocean Engineering Division, CSIR-National Institute of Oceanography (Council of Scientific & Industrial Research), Dona Paula, Goa - 403 004 India

<sup>2</sup>Coastal Processes & Shoreline Management, ICMAM- Project Directorate (Ministry of Earth Sciences), Chennai - 600 100 India

\*Corresponding author: Tel: 0091 832 2450 327 Fax: 0091 832 2450 602 Email: sanil@nio.org

### **Abstract**

We studied the wave characteristics before, during and after the onset of the Indian summer monsoon based on data measured using the buoy moored at 3 locations off the central west coast of India. The study reveals the dramatic changes that occur in wave field due to the monsoon. Mean significant wave height before the onset of the monsoon was 0.7-0.9 m and it increased to 2.4-2.6 m during the onset of monsoon at the locations studied. Before the monsoon, due to the sea breeze, the wave height increased and reached its peak at ~1100 UTC. Variation of wave height in one day was up to 2 m with the high values ( $> 1$  m) occurring during the monsoon. In contrast, the range of the peak wave period in one day varied up to 15 s before the monsoon due to the influence of the land breeze-sea breeze system. Also, before the monsoon, the spectral energy was in a wide range of frequencies due to the co-existence of swells and wind-seas, and 26% of the total spectral energy was in frequencies  $> 0.25$  Hz. Conversely, during the monsoon, only 7.1% of the total energy was in frequencies  $> 0.25$  Hz.

**Key words:** Ocean sciences, surface waves, spectral energy density, field data, diurnal variations

## 1. Introduction

The beaches along the west coast of India undergo seasonal erosion during the Indian summer monsoon (which lasts from June to September and hereafter is called “the monsoon”). The main factor responsible for this erosion is high wind waves generated by monsoon winds (Chandramohan et al., 1993). The average monsoon onset date over the southern part of Indian mainland is 1 June. During 2014, however, the monsoon was delayed and the onset date was 5 June (IMD, 2014). Strong cross-equatorial flow and intense westerlies over the Arabian Sea are the characteristic low-level features in the evolution process of the monsoon over India (Raju et al., 2005). Hence, it is important to know the changes in wave parameters during, before and after the onset of the monsoon. Kumar et al. (2010) studied the wave growth characteristics during a storm for a period of 7 days at a location off the west coast of India at a water depth of 14 m and observed that the maximum wave height increased from 2 to 8m within 60 h.

Generally, the sea state consists of one or several swells and wind-sea systems (Soares, 1991). Hence, the change in wave characteristics at a location can be either due to a change in the local winds or a change in remote swells. The different wave systems present at a location can be identified by analyzing the wave spectrum (Hanson and Phillips, 2001). Studies conducted in the eastern Arabian Sea indicate that the wave spectrum is bimodal due to the presence of wind-seas and swells (Baba et al., 1989; Kumar et al., 2003; Vethamony et al., 2011). The measurements of waves in the eastern Arabian Sea suggest that the significant wave heights ( $H_{m0}$ ) hardly exceed 5 m (Kumar et al., 2003; Kumar et al., 2010; Vethamony et al., 2011; Sajiv et al., 2012; Glejin et al., 2013; Kumar et al., 2014). The eastern Arabian Sea is relatively calm during the non-monsoon period (Glejin et al., 2013).

The present study examines the changes in the wave characteristics from 1 May to 19 July 2014 at three locations in the eastern Arabian Sea (Fig. 1). 1 May to 6 June 2014 is the period before the monsoon (also referred as pre-monsoon), 7 to 11 June 2014 is the period at the onset of the monsoon and 12 June to 19 July 2014 is the period after the onset of the monsoon. The paper is organized as follows. Section 2 contains the data and methodology used in the study. Section 3 contains a discussion of the results, and Section 4 summarizes the conclusions.

## 2. Methods

### 2.1 Study region

The study locations are; 1) off Vengurla at a water depth of 15 m in the eastern Arabian Sea (latitude 15.8327° N and longitude 73.5681° E), 2) off Honnavar at water depth of 30 m (14.307° N, 74.251° E) and 3) off Honnavar at 9 m water depth (14.304° N, 74.391° E) (Fig. 1). Honnavar is 250 km south of

Vengurla. The climate over the Arabian Sea is dynamic due to seasonally reversing monsoon winds (Kumar et al., 2012). The annual average significant wave height ( $H_{m0}$ ) of the eastern Arabian Sea is  $\sim 1$  m and the seasonal average is highest ( $\sim 2$  m) during the monsoon period (Kumar et al., 2014). Swells propagating from the southern hemisphere are present in the eastern Arabian Sea during the non-monsoon periods (Glejin et al., 2013). The east side of this coastal segment is bound by the Western Ghats mountain range, while the Arabian Sea extends along its west side. The tidal range at Vengurla is 2.3 m during the spring tide and 1.3 m during the neap tide, and the tides are predominantly semi-diurnal and mixed. Kumar and Kumar (2008) reported that the  $H_{m0}$  up to 5.7 m is measured during monsoon at 23 m water depth at a location 55 km south of the Vengurla buoy location. Based on Davis's classification (1964) and Short's criteria (2012), the wave and tide data together exhibit that the study area is in a micro-tidal wave dominated coast. The study region receives rainfalls of 800, 1200, 1200 and 300 mm from June to September (Ratna, 2012).

## 2.2 Data and methodology

Wave data measured using the Datawell directional wave rider buoys from 1 May 2014 to 19 July 2014 were used in the study. The significant wave height ( $H_{m0}$ ), the mean wave period ( $T_{m02}$ ) and the peak wave period ( $T_p$ ) were estimated from the wave spectrum. The mean wave direction (MWD) corresponding to the peak frequency ( $f_p$ ) was estimated based on circular moments (Kuik et al., 1988). The details of the data analysis are similar to that presented in Kumar et al. (2014). From the half hourly wave spectra, the average wave spectrum for the required period was computed by taking the average of the spectral energy density at the respective frequencies. Similarly 99, 90, 75 and 50 percentile wave spectra were also computed from the half hourly wave spectra. The different percentile lines indicate how often the energy was below a particular value at different frequencies. For example, a 99 percentile line indicates that 99% of the wave spectra fell below this line.

The wind-seas and swells from the measured wave data were separated through a 1-D separation algorithm (Portilla et al., 2009), on the basis of the assumption that, the energy at the peak frequency of a swell system cannot be higher than the value of a PM spectrum (Pierson and Moskowitz, 1964) with the same peak frequency. It calculates the ratio ( $\gamma^*$ ) between the peak energy of a wave system and the energy of a PM spectrum at the same frequency. If  $\gamma^*$  is above a threshold value of 1, the system is considered to represent wind-sea, else it is taken to be swell. Wind-sea and the swell parameters were computed by integrating over the respective spectral parts.

Since no measured wind data are available for the study location, to analyse the wind pattern, the zonal and meridional components of the wind speed at a height of 10 m in 6 hour intervals from NCEP/NCAR (Kalnay et al., 1996) which is at a coarse resolution ( $2.5^\circ \times 2.5^\circ$ ) is used. These data were provided by the NOAA-CIRES Climate Diagnostics Center, Boulder, Colorado at <http://www.cdc.noaa.gov/>.

### **3. Results and discussion**

#### **3.1 Bulk wave parameters**

The onset of the south-west monsoon season is marked by (1) the establishment of a south-western airflow over the Arabian Sea, (2) intensifying surface winds and (3) a cross equatorial airflow at  $40\text{-}60^\circ$  E flowing toward the Indian west coast as strong westerlies (Pawar et al., 2005). The low-level jet with surface winds of 10-12 m/s advances eastward and slowly covers the whole of the latitudinal belt from  $7^\circ$  to  $13^\circ$  N over the Arabian Sea. Such strong winds create waves (Pawar et al., 2005). During the monsoon season, the average winds over the Arabian Sea are always strong, but they fluctuate over a large range at a specific location (Pawar et al., 2005). Off Vengurla during the study period, the highest individual wave height before the monsoon was 2 m and the average height of the waves was 0.4 m. During the onset of the monsoon (1 May to 6 June), the highest wave height was 7 m with an average value of 1.3 m at Vengurla. Before the monsoon, only 1.9% of the waves were higher than 1 m, while during the monsoon, 60% of the waves were higher than 1 m. The mean  $H_{m0}$  before the onset of the monsoon was 0.7 m. Due to the influence of the monsoon, the  $H_{m0}$  increased from 1 m on 7 June 2014 and reached a maximum of 4.5 m on 11 June 2014. From 7 to 11 June, the average  $H_{m0}$  was 2.4 m. This increase in  $H_{m0}$  was in accordance with the increase in wind speed (Fig. 2a). Before the monsoon, the wind speed was less than 4 m/s, but during the onset of the monsoon, the wind speed increased up to 15 m/s. After the initial increase, there was a decrease in the  $H_{m0}$  due to a decrease in the wind speed. After the onset of the monsoon, the average  $H_{m0}$  was similar to its value during the onset of the monsoon ( $\sim 2.4$  m).

Off Honnavar, at both the 30 and 9 m water depth, the change in the wave characteristics due to the monsoon was similar to that at observed at Vengurla (Fig. 3). Off Honnavar, the mean  $H_{m0}$  before the onset of the monsoon was higher ( $\sim 0.9$  m) at both 30 m and 9 m water depth than that ( $\sim 0.7$  m) at Vengurla. During the monsoon, maximum  $H_{m0}$  was higher ( $\sim 4.5$  m) at Vengurla than at Honnavar ( $\sim 4.2$  m), but the mean  $H_{m0}$  during monsoon was higher ( $\sim 2.6$  m) at Honnavar than at Vengurla ( $\sim 2.4$  m) (Fig. 4).  $H_{m0}$  at 30 m water depth was around 10% higher than that at 9 m water depth.

The average value of the mean wave period increased from 5 s during the pre-monsoon to 7 s during the monsoon, whereas during the same time periods, the average value of the peak wave period decreased from 12.5 s to 11.5 s at Vengurla (Fig. 2), from 13.1 to 11.3 s at 30 m water depth off Honnavar and from 13.7 to 11.7 s at 9 m water depth off Honnavar (Fig. 3). Even though there will be long period swells during the monsoon, due to the interaction of monsoonal waves (immature swells) with long period swells, the frequency of the peak wave energy slightly moved towards the high frequency region (Fig. 5). Hence, the decrease in peak wave period was due to the reduction in long period swells during the monsoon. The comparison of wave parameters at Vengurla and Honnavar before the monsoon shows that there was large variation in  $T_{m02}$  and mean wave direction due to the influence of local winds, but during the monsoon the variation in wave parameters at these locations were within 10 to 15% (Figs. 4a to 4c). Similarly, the comparison of wave parameters at 9 and 30 m water depth off Honnavar shows that the variation in wave parameters during the pre-monsoon period is larger than that during the monsoon period (Figs. 4d to 4f).

Since the mean wave period increased, the number of waves within a 30 minute period decreased from 369 to 258 from the pre-monsoon to the monsoon. Before the monsoon, the waves were predominantly swells with a  $T_p$  ranging from 10 to 18 s. During the monsoon, the  $T_p$  was within 10 to 14 s. Waves with a peak period of 3 to 8 s from the north-west were also observed before the monsoon, but these waves were absent during the monsoon period (Figs. 2b & 2d). The north-west waves before the monsoon are the wind-seas due to the winds (sea breeze) from the north-west and the short period swells by the Shamal events (Fig. 2d). In May (before the monsoon), Glejin et al. (2013) reported presence of north-west waves off Ratnagiri, 130 km north of the Vengurla buoy location due to the Shamal events.

During the pre-monsoon period, long period swells ( $T_p \sim 18$  s) arrived in distinct trains lasting about 5 days. In addition to the trains of swells, five episodes of higher frequency waves from the north-west occurred. During May 2009, Kumar et al. (2012) also observed the arrival of swells ( $T_p > 10$  s) in distinct trains lasting about 5 days off the west coast of India at locations situated 125 and 300 km south of the present study location.

During the onset of the monsoon, the wave steepness increased rapidly, and after reaching a maximum value of 0.056, the steepness decreased due to an increase in the wave period with an increase in the wave height (Fig. 2c). Before the onset of the monsoon, the diurnal variation in wave steepness was large since the mean wave period and  $H_{m0}$  exhibited diurnal variation during the pre-monsoon. The same pattern was not observed during the monsoon (Fig. 2c). Earlier studies off the west coast of India indicated diurnal variation in wave parameters due to the influence of the sea breeze (Neetu et al., 2006;

Vethamony et al., 2011; Glejin et al., 2013; Kumar et al., 2014). Along the west coast of India, the sea breeze starts around 0530 UTC (1100 Local Time), and it continues to blow in the NW direction with a maximum wind speed of between 0930 UTC (1500 LT) and 1230 UTC (1800 LT). After this, the wind speed gradually reduces (Vethamony et al., 2011). In this study off Vengurla, before the monsoon, the wave height increased and reached its peak at ~ 1100 UTC (1630 LT) due to the sea breeze. After this, the wave height decreased and swell conditions prevailed by 1800 UTC (Fig. 6). Off Honnavar, before the monsoon, the wave height was minimum at 0800 UTC and started increase from 1100 UTC and reached its peak at 1600-1800 UTC (Fig. 7). The wave height and the wave periods (both the mean wave period and the peak wave period) show an inverse proportion before the monsoon at all the locations studied, but such a relation was not found during the onset of the monsoon or during the monsoon period. Vethamony et al. (2011) showed that, off the Goa coast, the superimposition of locally generated waves from the NW with a pre-existing swell from the SW leads to an obvious increase in wave height.

In this study, the range of  $H_{m0}$  (the difference between the maximum and the minimum value) in one day varied up to 2 m with the high values ( $> 1$  m) occurring during the monsoon period (Fig. 8a). The range of the  $T_{m02}$  in one day varied up to 3 s with the high values ( $> 2$  s) occurring mainly during the pre-monsoon period (Fig. 8b). During this period, the range of the  $T_p$  in one day varied up to 15 s (Fig. 8c). The large variation in the  $T_{m02}$  and the  $T_p$  in one day before the monsoon was due to the influence of the land breeze-sea breeze system. During the land breeze period, swells were predominant, while during the sea breeze period, wind-seas were predominant. Also, due to the influence of land/sea breezes, the mean wave direction varied up to  $150^\circ$  in a day during the pre-monsoon period (Fig. 8d). The parameter influencing the direction of the longshore sediment transport along the coast is the mean direction. Since there was a large variation in the mean wave direction in one day, it is important to consider the wave parameters at hourly intervals while studying the coastal processes.

The joint distribution of the significant wave height and the mean wave direction indicate three peaks: one corresponding to the south-west swells, the second corresponding to the north-west waves during the pre-monsoon period (1 May- 6 June) and the third corresponding to the south-west-westerly waves during the monsoon (Fig. 9). Even though the winds in the eastern Arabian Sea are from the south-west during the monsoon, the waves roll south-west-westerly due to the refraction and the high waves ( $H_{m0} > 4$  m) roll almost perpendicular to the coast. Hence, the spread in wave direction is less at 15 and 9 m water depth compared to 30 m water depth (Fig. 9).

During the study period, the average contribution of short period waves ( $T < 6$  s; dominated by local seas) was 43% before the onset of the monsoon. These waves were reduced to 19% due to the monsoon

(Fig. 5). The contribution of long period waves ( $T > 12$  s; resulting primarily from swell) changed from 20 to 18%, and the contributions of intermediate period waves changed from 37 to 63% due to the monsoon. During the monsoon, predominantly intermediate period waves were observed.

In open and large oceanic regions, there usually is a predominance of swell fields generated by strong remote storms. In the gulfs and bays, although mixed-seas are frequently observed, there is a predominance of wind-seas (Hwang et al., 2011). Based on data from five field campaigns to study the influence of wave age on the air-sea momentum flux during pure wind-sea conditions, Drennan et al. (2003) found that pure wind-seas are frequent in coastal regions, in enclosed seas and during extreme wind events. However, in the open ocean, swell is usually present. Wind-seas, as expected, should be highly correlated to the local winds. In a particular location, both swells and wind-seas can and do co-exist, but a predominance of one or the other is normally found. Most of the time, a mixture of swell and wind-sea is present in the wave spectrum. The correlation between  $U/gT_p$  and  $U^2/gH_{m0}$  (Fig.10) is one method for analysing swell/wind-sea regimes. The dashed line represents the theoretical curve based on the following expression for a fully developed wind-sea, as given by Hasselmann et al. (1976). The points far off the theoretical, fully developed wind-sea curve correspond to a wide range of swell fields found in the study region.

$$\frac{U}{gT_p} = 4.8 \times 10^{-2} \left( \frac{U^2}{gH_{m0}} \right)^{0.66} \quad (1)$$

During the study period, the wind-sea from the SW and the W were mainly under the fully-developed condition, whereas the wind-sea from the NW deviated from the theoretical curve for fully developed conditions due to the short fetch (Fig. 10). Kumar et al. (2014) observed that the wave data off the west coast of India fall slightly below the theoretical fully developed wind-sea curve due to the presence of swells in the region.

### 3.2 Wave spectrum

In order to understand the evolution of spectral components over time, the contour plots of wave spectral energy density in a frequency-time domain are analyzed. Since the maximum spectral energy density of each record varied from 0.2 to 70.3  $m^2/Hz$  during the study period, the contour plots of spectral energy density are presented in a logarithmic scale (Fig. 11a). Before the monsoon, the spectral energy was spread to higher frequencies ( $> 0.25$  Hz) and 26% of the total spectral energy was beyond 0.25 Hz at Vengurla and 19% at Honnavar. During the monsoon period, 92.6% of the total spectral energy was

within 0.05 to 0.25 Hz and only 7.1% of the total energy was spread in frequencies greater than 0.25 Hz at all the locations.

Both swell and wind-sea dominated spectra were observed in the study area and the typical wave spectra during the study period are presented in Fig. 12. Before the monsoon, 71% of the wave spectra were multi-peaked and 64% of the total spectra were swell-dominated. During the onset of the monsoon, single-peaked spectra increased from 29% to 51% and were mainly swell-dominated. A noteworthy feature is the dominance of swells (~51%) during the onset of the monsoon. During this period, the dominance of seas is expected along the west coast of India due to prevailing high winds all over the Arabian Sea. Kumar et al. (2012) observed swell dominance (72%) off the west coast of India during the monsoon period. In the present study, during the monsoon, 77% of the spectra off Vengurla were single-peaked and all of them were swell-dominated.

The averaged wave spectra and the 99, 90, 75 and 50 percentile wave spectra before the monsoon show the predominant peak at 0.075 Hz, a secondary peak at 0.11 Hz and a wind-sea peak at 0.26 Hz (Fig. 13). During the onset of the monsoon, the peak of the averaged and the 99, 90, 75 and 50 percentile wave spectra varied from 0.075 to 0.091 Hz, and the spectra were single-peaked. During the growth, nonlinear wave-wave interaction transferred energy from the spectral peak region to both the lower and higher frequencies and broadened the wave spectrum. After the onset of the monsoon, the peaks of all averaged spectra were around 0.08 Hz and the spectra were single-peaked.

Waves with  $H_{m0} > 2$  m were observed 63% of the time during the monsoon and 57% during the onset of the monsoon. Before the monsoon, the highest  $H_{m0}$  is 1.2 m and the  $H_{m0}$  exceeded 1 m only 3% of the time. In contrast, during the monsoon, the  $H_{m0}$  was more than 1 m all the time. Kumar and Kumar (2008) represented the shallow water wave spectrum of high waves ( $H_{m0} > 2$  m) with a JONSWAP spectrum (Hasselmann et al., 1973) with modified  $\alpha$  (Phillips constant) and peak enhancement ( $\gamma$ ) parameters ( $\alpha=0.0027$  and  $\gamma =1.63$ ). Since these high wave spectra along the eastern Arabian Sea are mainly swells and are narrow spectra, the JONSWAP spectrum with appropriate  $\gamma$  can represent the swell spectra (Goda, 1983). This study shows that a spectrum of high waves ( $H_{m0} > 2$  m) could be represented with the JONSWAP spectrum (Fig. 11). A fitted JONSWAP spectrum is obtained by selecting the parameter  $\alpha$  and  $\gamma$  of the JONSWAP spectrum such that the peak of the spectrum agrees. The estimated values of the JONSWAP parameters for all the 3 locations are less than the generally recommended values of 0.0081 and 3.3, respectively. The high frequency part of the spectrum is not represented well with the JONSWAP spectrum especially at the 30 m water depth off Honnavar. Due to



dissipation, the spectral energy density for frequency more than 0.1 Hz was less at 9 m water depth compared to 30 m water depth (Figs. 14b and 14c). Kumar and Anjali (2015) observed that the high-frequency part of the spectra of high waves ( $H_{m0} > 2$  m) is between the curves proportional to  $f^4$  and  $f^3$  (where  $f$  is the frequency). For frequencies from 0.1 Hz to 0.2 Hz, the high-frequency part is close to  $f^3$ , and for frequencies from 0.2 Hz to 0.4 Hz, the high-frequency part is close to  $f^4$ . Young and Verhagen (1996) found that the exponent of the spectral curve in the high-frequency region is approximately -5 in deep water and around -3 in finite depth.

During the study period, the mean wave direction of waves with frequencies of 0.06 to 0.15 Hz before the onset of the monsoon was between 210 and 240° (Fig. 11b). During the monsoon, the direction of these waves changed to 240 to 270°. Before the onset of the monsoon and the monsoon, waves with the frequency 0.15 to 0.4 Hz were mainly from 270 to 300°. During the monsoon, these waves were also mainly from 240 to 270°. Some waves with a direction of more than 300° were also observed before the monsoon, but those waves were not observed during the monsoon. During the monsoon, low-frequency ( $< 0.07$  Hz) waves ranged from 210 to 240°.

#### **4. Conclusion**

The analysis of open ocean wave observations in the presence of background swell before, during and after the onset of the Indian summer monsoon was conducted based on data measured at a water depth of 15 m off Vengurla, India from 1 May to 19 July 2014. Due to the monsoon influence, the significant wave height increased from 1 m on 7 June 2014 and reached a maximum of 4.5 m on 11 June 2014. The variation of significant wave height in one day was high ( $> 1$  m) during the monsoon and the variation of peak wave period in one day was high ( $\sim 15$  s) during the pre-monsoon period due to the influence of land/sea breezes. The diurnal variation in wave steepness was large before the onset of the monsoon since the mean wave period and the  $H_{m0}$  exhibited diurnal variation during the pre-monsoon. The same pattern was not observed during the monsoon. Before the monsoon, the average wave spectra and the 99, 90, 75 and 50 percentile wave spectra showed two peaks in the swell region (a predominant peak at 0.075 Hz and a secondary peak at 0.11 Hz) and a wind-sea peak at 0.26 Hz. After the onset of the monsoon, the spectra were single-peaked with the peaks of the average spectra at around 0.08 Hz.

#### **Acknowledgments**

The authors gratefully acknowledge the financial support given by the Council of Scientific & Industrial Research, New Delhi and Earth System Science Organization, Ministry of Earth Sciences, Government of India to conduct part of this research. Director, CSIR-NIO, Goa provided encouragement to carry out the study. We thank both the reviewers for their critical comments and the suggestions for additional studies which improved the paper. This is NIO contribution No. 2015.

## References

- Baba, M., Dattatri, J., Abraham, S., 1989. Ocean wave spectra off Cochin, west coast of India, *Indian J. Mar. Sci.* 18, 106-112.
- Chandramohan, P., Nayak, B.U., Kumar, V. S., Pathak, K.C., 1994. Beach processes between Mulgund and Shiroda, west coast of India, *Indian J. Mar. Sci.*, 23, 102-104.
- Davies, J.L., 1964. A morphogenic approach to world shorelines. *Zeitschrift fur Geomorphology*, 8, Mor-tensen Sonderheft, pp 127-142.
- Drennan, W.M., Graber, H.C., Hauser, D., Quentin, C., 2003. On the wave age dependence of wind stress over pure wind seas. *J Geophys Res* 108, 8062, doi:10.1029/2000JC000715
- Glejin, J., Kumar, V.S., Nair, T.N.B., Singh, J., 2013. Influence of winds on temporally varying short and long period gravity waves in the nearshore regions of the eastern Arabian Sea, *Ocean Sciences* 9, 343–353.
- Goda, Y., 1983. Analysis of wave grouping and spectra of long-travelled swell. Japan: Rep. Port Harbour Res. Inst. 22, pp. 3-41.
- Hanson, J.L. and Phillips, O.M., 2001, Automated analysis of ocean surface directional wave spectra, *J. Atmos. Oceanic. Technol.*, 18, 277–293.
- Hasselmann, K., Barnett, T.P., Bouws, E., Carlson, H., Cartwright, D.E., Enke, K., Ewing, J.A., Gienapp, H., Hasselmann, D.E., Kruseman, P., Meerburg, A., Muller, P., Olbers, D.J., Richter, K., Sell, W., Walden, H., 1973. Measurements of wind-wave growth and swell decay during the Joint North Sea Wave Project (JONSWAP), *Deutsche Hydrograph. Z.* A12, 95.
- Hasselmann, K., Ross, D.B., Miller, P., Sell, W. 1976. A parametric wave prediction model. *J Phys. Oceanogr.* 6, 200-228
- Hwang, P. A., Garcia-Nava, H., Ocampo-Torres, F. J., 2011, Dimensionally Consistent Similarity Relation of Ocean Surface Friction Coefficient in Mixed Seas, *J. Phys. Oceanogr.*, 41, 1227–1238.
- IMD, 2014, Monsoon - 2014 onset over Kerala, Press Release India Meteorological Department, [http://www.imd.gov.in/section/nhac/dynamic/Monsoon\\_frame.htm](http://www.imd.gov.in/section/nhac/dynamic/Monsoon_frame.htm) ( accessed on 10 October 2014)
- Kalnay, E., Kanamitsu, M., Kistler, R., Collins, W., Deaven, D., Gandin, L., Iredell, M., Saha, S., White, G., Woollen, J., Zhu, Y., Leetmaa, A., Reynolds, B., Chelliah, M., Ebisuzaki, W., Higgins, W., Janowiak, J., Mo, K.C., Ropelewski, C., Wang, J., Jenne, R., Joseph, D., 1996. The NCEP/NCAR 40-year reanalysis project. *Bulletin of the American Meteorological Society* 77, 437-471.
- Kuik, A.J., Vledder, G., Holthuijsen, L.H., 1988. A method for the routine analysis of pitch and roll buoy wave data. *J. Phys. Oceanogr.* 18(7), 1020–1034.
- Kumar, V.S., Anand, N.M., Kumar, K.A., Mandal, S., 2003. Multi-peakedness and groupiness of shallow water waves along Indian coast. *J. Coastal. Res.* 19, 1052-1065.
- Kumar, V.S., Anjali, N.M., 2015, Inter-annual variations in wave spectral characteristics at a location off the central west coast of India, *Ann. Geophys.* 33, 159-167.

- Kumar, V.S., Johnson, G., Dora, G.U., Philip, S.C., Singh, J., Pednekar, P., 2012. Variations in nearshore waves along Karnataka, west coast of India, *J. Earth. Syst. Sci.*, 121, 393-403.
- Kumar, V.S., Kumar, K.A., 2008. Spectral representation of high shallow water waves. *Ocean Eng.*, 35, 900-911.
- Kumar, V.S., Philip, S., Nair, T.N.B., 2010. Waves in shallow water off west coast of India during the onset of summer monsoon. *Ann. Geophys.* 28, 817–824.
- Kumar, V.S., Shanas, P.R., Dubhashi, K.K., 2014. Shallow water wave spectral characteristics along the eastern Arabian Sea, *Natural Hazards* 70, 377–394, DOI 10.1007/s11069-013-0815-7.
- Neetu, S., Shetye, S.R., Chandramohan, P., 2006, Impact of sea-breeze on wind-seas off Goa, west coast of India, *J. Earth Syst. Sci.*, 115(2), 229–234.
- Pawar, S.D., Siingh, D., Gopalakrishnan, V., Kamra, A.K., 2005. Effect of the onset of southwest monsoon on the atmospheric electric conductivity over the Arabian Sea, *J. Geophys. Res.*, 110, D10204, doi:10.1029/2004JD005689.
- Pierson, W.J., Moskowitz, L., 1964. A proposed form for fully developed seas based on the similarity theory of S.A. Kitaigorodski. *J. Geophys. Res.* 69, 5181-5190.
- Portilla, J., Ocampo-Torres, F.J., Monbaliu, J., 2009. Spectral Partitioning and Identification of Wind Sea and Swell. *J. Atmos. Ocean Tech.* 26, 117-122.
- Raju, P.V.S., Mohanty, U.C., Bhatla, R., 2005. Onset characteristics of the southwest monsoon over India, *International Journal of Climatology*, 25, 167-182.
- Ratna, S., B., 2012. Summer Monsoon Rainfall Variability Over Maharashtra, India, *Pure Appl. Geophys.* 169, 259–273.
- Sajiv, P.C., Kumar, V.S., Glejin, J., Udhaba, D.G., Vinayaraj, P., 2012. Interannual and seasonal variations in nearshore wave characteristics off Honnavar, west coast of India, *Curr. Sci.*, 103, 286-292.
- Short, A.D., 2012. Coastal processes and beaches, *Nature education knowledge*, 3(10), 15.
- Soares, C.G., 1991, On the occurrence of double peaked wave spectra. *Ocean Eng.* 18(1/2), 167-171.
- Vethamony, P., Aboobacker, V.M., Menon, H.B., AshokKumar, K., Cavaleri, L., 2011. Super imposition of wind seas on pre-existing swells off Goa coast. *J. Mar. Syst.* 87 (1), 47–54.
- Young, I.R., Verhagen, L.A., 1996. The growth of fetch limited waves in water of finite depth. Part I: Total energy and peak frequency, *Coastal Eng.*, 29, 47–78.

## Figure Captions

Figure 1. Map showing the study locations. One location is off Vengurla at 15 m water depth and two locations are off Honnavar at 9 and 30 m water depth. The shadings are the depth in m. Map is plotted using ocean data viewer

Figure 2. Time series plot of a) significant wave height ( $H_{m0}$ ) and wind speed, b) peak wave period ( $T_p$ ), c) wave steepness and d) mean wave direction (MWD) and wind direction from 1 May to 19 July 2014 off Vengurla

Figure 3. Time series plot of a) significant wave height ( $H_{m0}$ ) and wind speed, b) peak wave period ( $T_p$ ), c) wave steepness and d) mean wave direction (MWD) and wind direction from 1 May to 19 July 2014 off Honnavar at 9 and 30 m water depth

Figure 4. Scatter plot of a) significant wave height, b) mean wave period and c) mean wave direction at Vengurla and Honnavar at 9 m water depth, d) significant wave height, e) mean wave period and f) mean wave direction at Honnavar at 9 m and 30 m water depth

Figure 5. Time series plot of percentage of long, intermediate and short period waves off a) Vengurla, b) Honnavar at 30 m water depth and c) Honnavar at 9 m water depth

Figure 6. Hourly variation of significant wave height and mean wave period (Left panel) and significant wave height of wind-sea and peak wave period (right panel) from 1 May to 6 June, 7 to 11 June and 12 June to 19 July 2014 off Vengurla. The time is in UTC

Figure 7. Hourly variation of significant wave height and mean wave period (Left panel) and significant wave height of wind-sea and peak wave period (right panel) from 1 May to 6 June, 7 to 11 June and 12 June to 19 July 2014 off Honnavar a) at 30 m water depth and b) at 9 m water depth. The time is in UTC

Figure 8. Range of wave parameters off Vengurla in a day a) significant wave height ( $H_{m0}$ ), b) mean wave period ( $T_{m02}$ ), c) peak wave period ( $T_p$ ) and d) mean wave direction (MWD) from 1 May to 19 July 2014

Figure 9. Joint distribution of significant wave height ( $H_{m0}$ ) and mean wave direction (MWD) from 1 May to 19 July 2014 a) off Vengurla at 15 m water depth, b) off Honnavar at 30 m water depth and c) off Honnavar at 9 m water depth

Figure 10. Plot of  $\log(U/gT_p)$  versus  $\log(U^2/gH_{m0})$  for wind-sea for the data measured before, during and after the onset of monsoon at Vengurla. Dashed line represents the theoretical relation given by Eq. 1.

Figure 11. Contour plots of a) spectral energy density with frequency and b) mean wave direction with frequency from 1 May to 19 July 2014 off Vengurla

Figure 12. Typical single and multi peaked wave spectra during the study period off Vengurla

Figure 13. Averaged and the 99, 90, 75 and 50 percentile wave spectra during a) 1 May - 6 June, b) 7-11 June and c) 12 June-19 July off Vengurla

Figure 14. Average wave spectrum during onset of monsoon (left panel) and during monsoon (right panel) off Vengurla and off Honnavar. The fitted JONSWAP spectrum is also shown

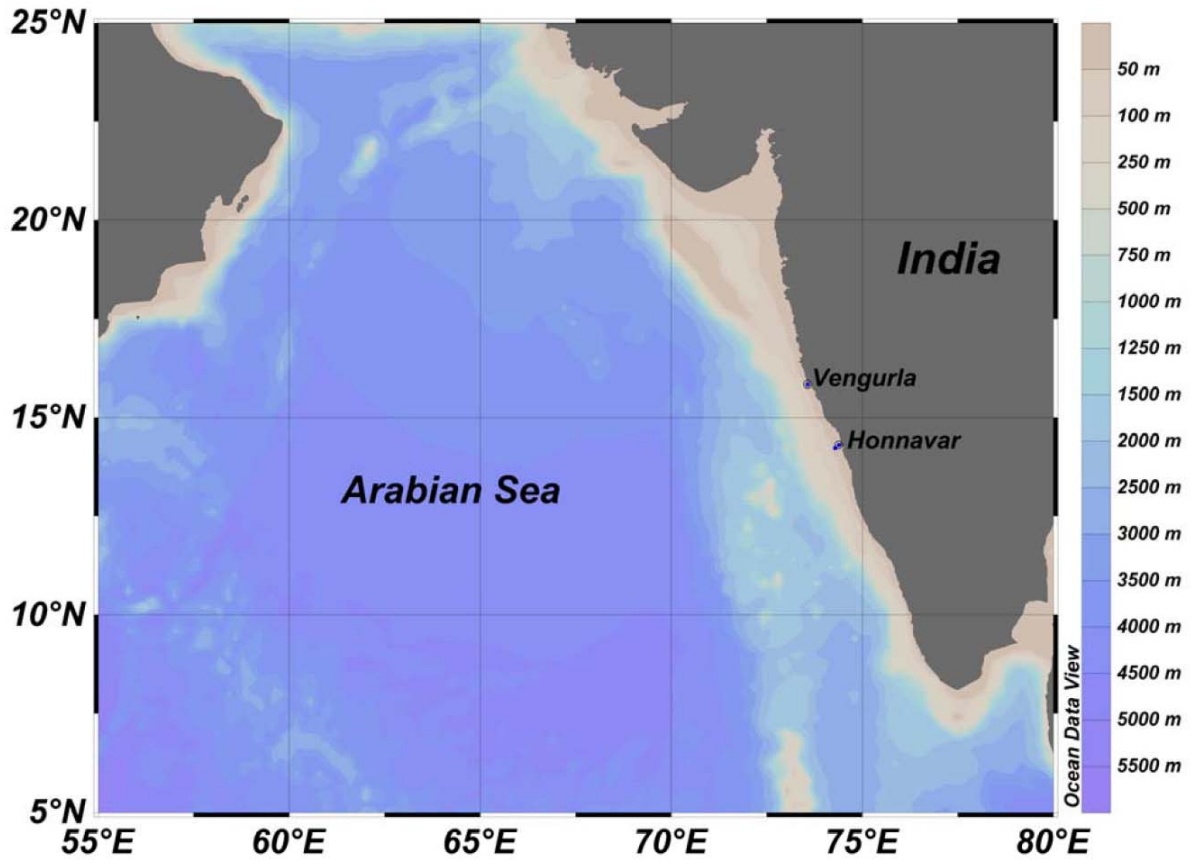


Figure 1. Map showing the study locations. One location is off Vengurla at 15 m water depth and two locations are off Honnavar at 9 and 30 m water depth. The shadings are the depth in m. Map is plotted using ocean data viewer.

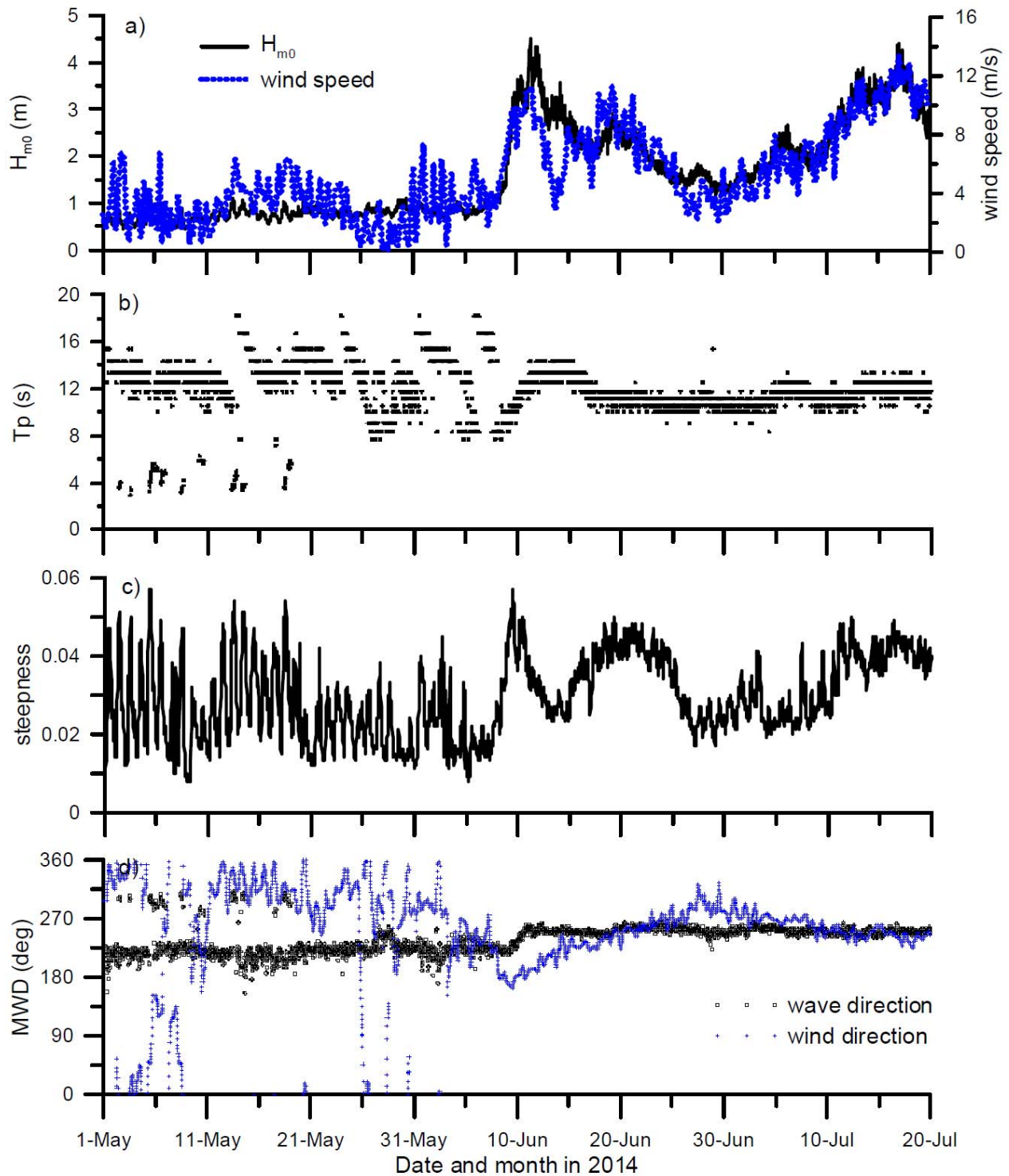


Figure 2. Time series plot of a) significant wave height ( $H_{m0}$ ) and wind speed, b) peak wave period ( $T_p$ ), c) wave steepness and d) mean wave direction (MWD) and wind direction from 1 May to 19 July 2014 off Vengurla

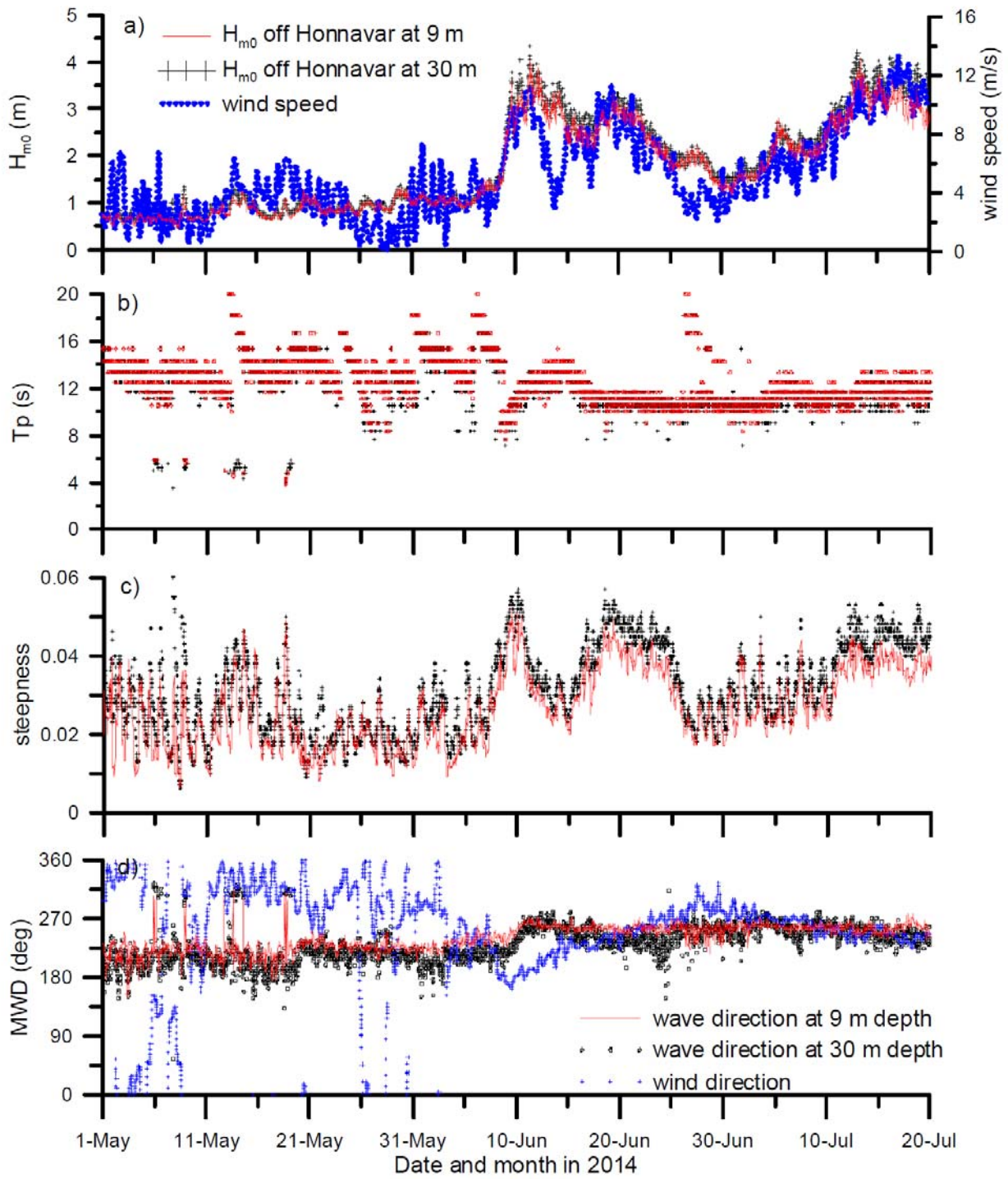


Figure 3. Time series plot of a) significant wave height ( $H_{m0}$ ) and wind speed, b) peak wave period ( $T_p$ ), c) wave steepness and d) mean wave direction (MWD) and wind direction from 1 May to 19 July 2014 off Honnavar at 9 and 30 m water depth

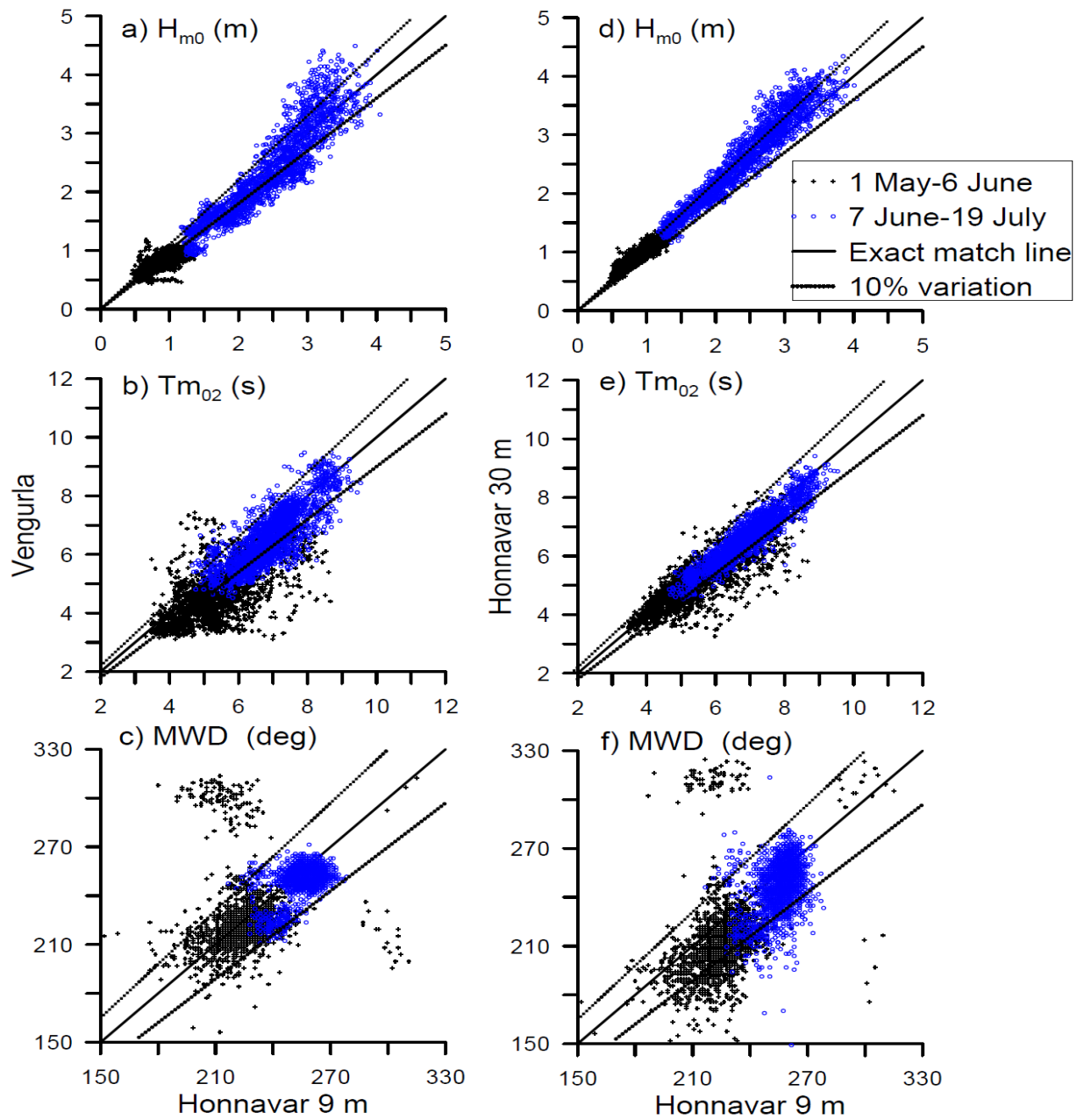


Figure 4. Scatter plot of a) significant wave height, b) mean wave period and c) mean wave direction at Vengurla and Honnavar at 9 m water depth, d) significant wave height, e) mean wave period and f) mean wave direction at Honnavar at 9 m and 30 m water depth



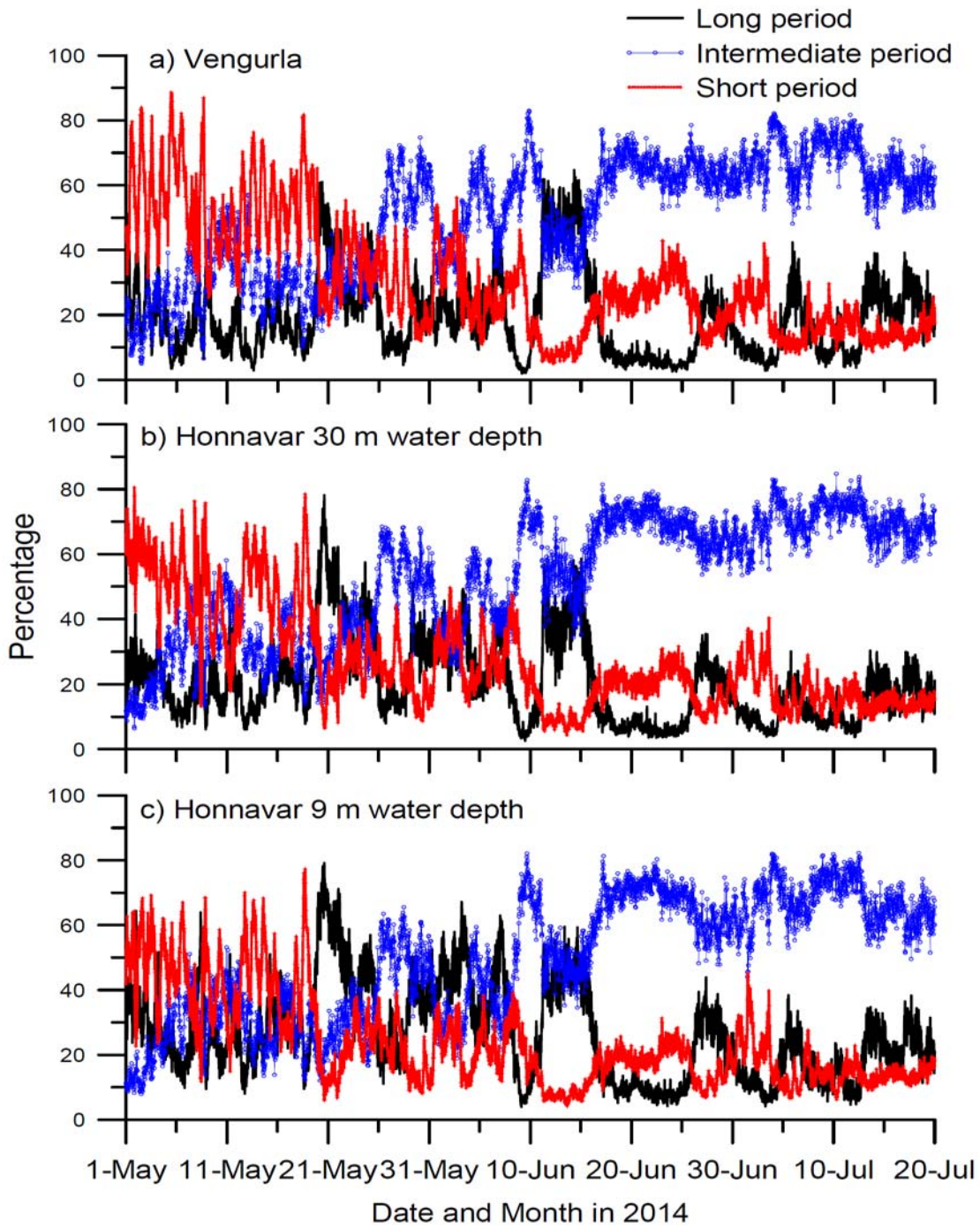


Figure 5. Time series plot of percentage of long, intermediate and short period waves off a) Vengurla, b) Honnavar at 30 m water depth and c) Honnavar at 9 m water depth

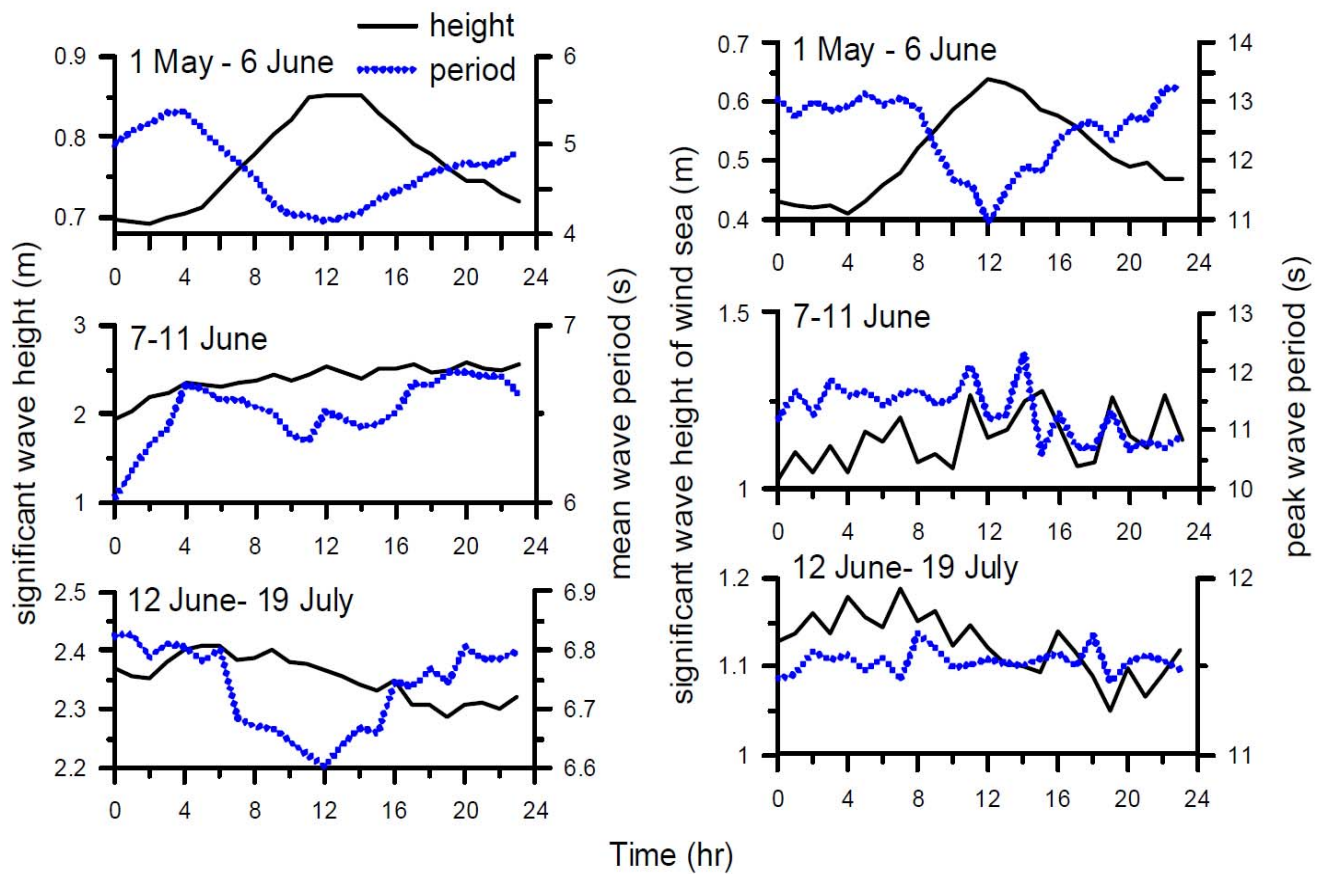


Figure 6. Hourly variation of significant wave height and mean wave period (left panel) and significant wave height of wind-sea and peak wave period (right panel) from 1 May to 6 June, 7 to 11 June and 12 June to 19 July 2014 off Vengurla. The time is in UTC.

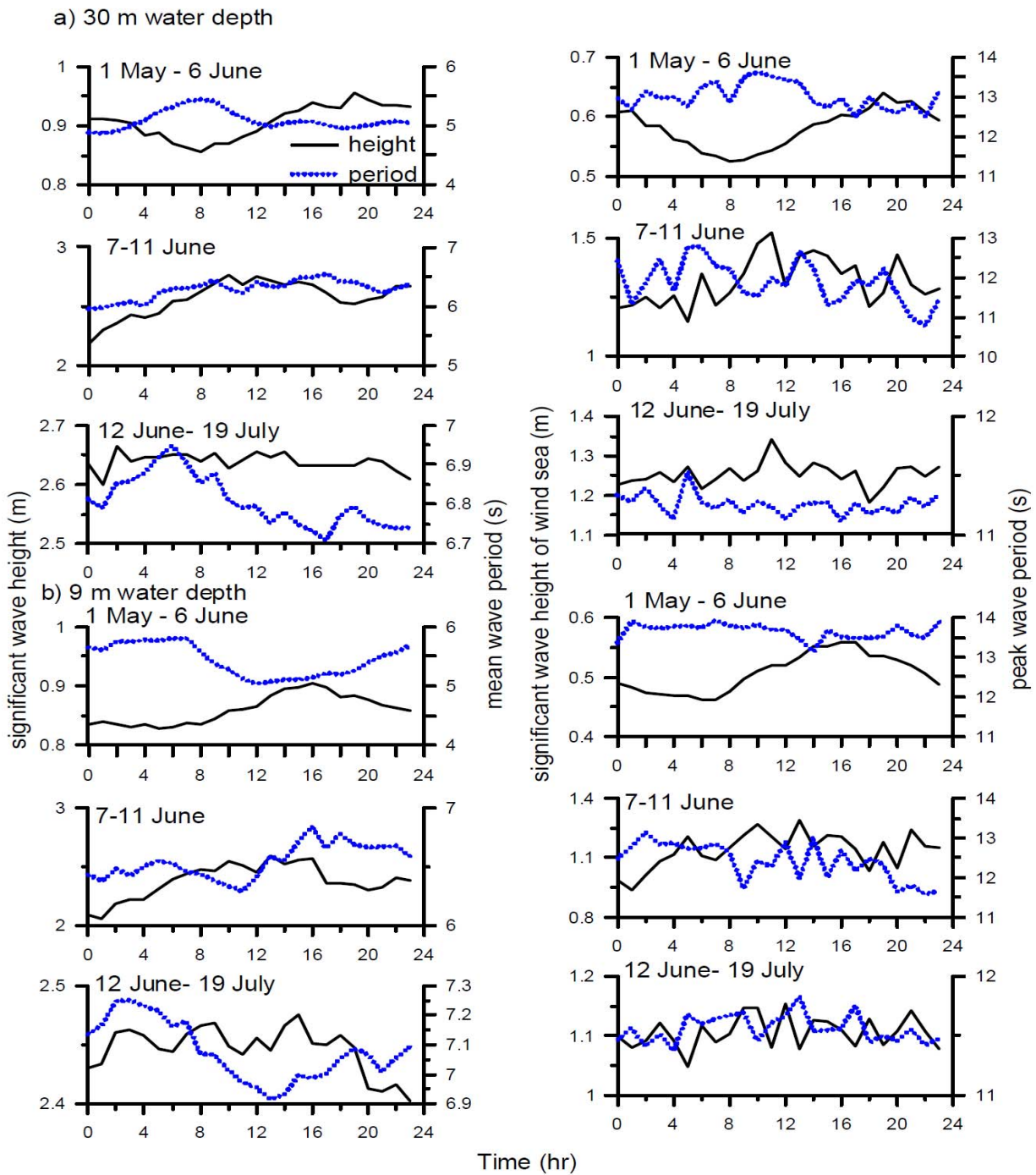


Figure 7. Hourly variation of significant wave height and mean wave period (Left panel) and significant wave height of wind-sea and peak wave period (right panel) from 1 May to 6 June, 7 to 11 June and 12 June to 19 July 2014 off Honnavar a) at 30 m water depth and b) at 9 m water depth. The time is in UTC

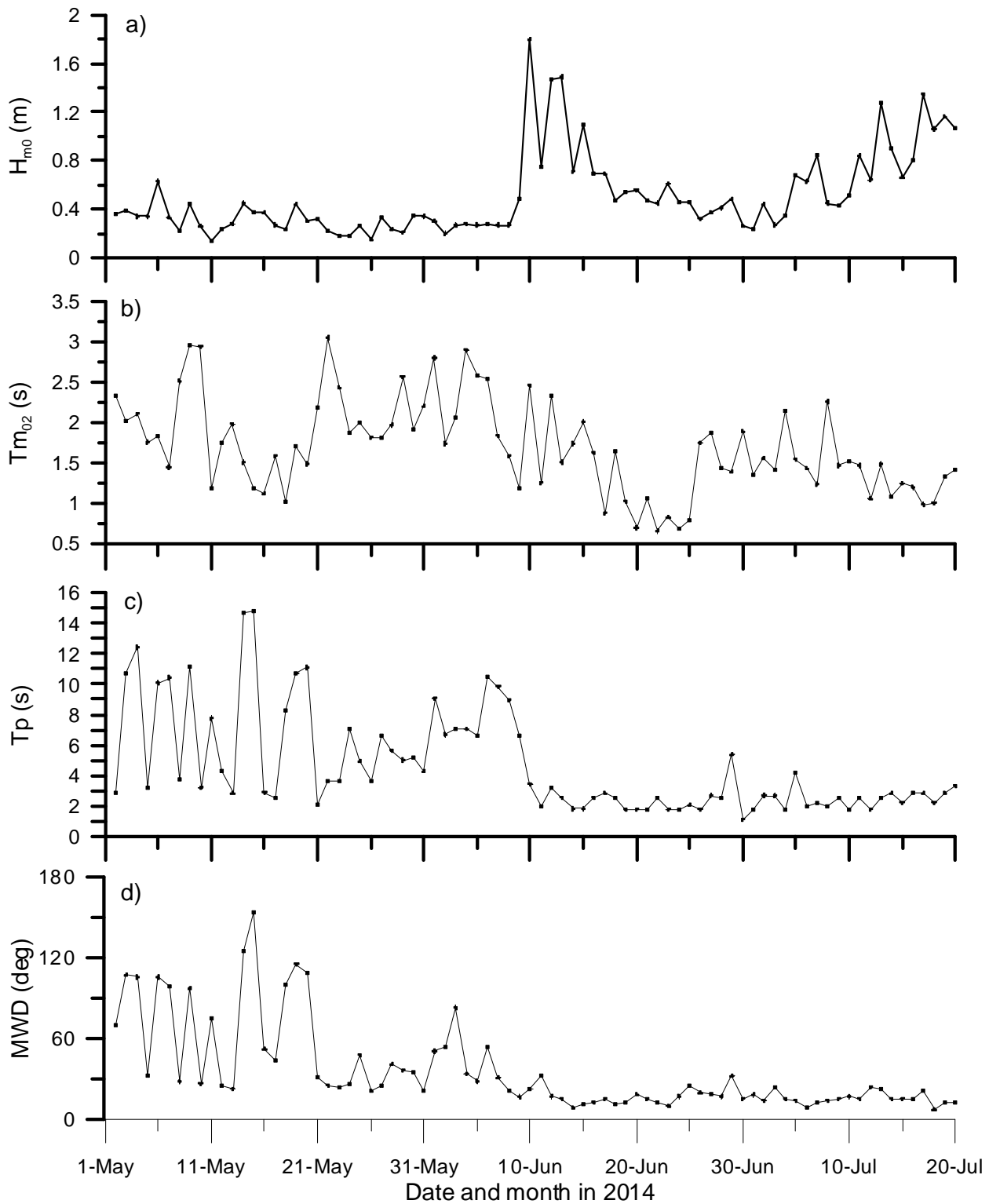


Figure 8. Range of wave parameters off Vengurla in a day a) significant wave height ( $H_{m0}$ ), b) mean wave period ( $T_{m02}$ ), c) peak wave period ( $T_p$ ) and d) mean wave direction (MWD) from 1 May to 19 July 2014

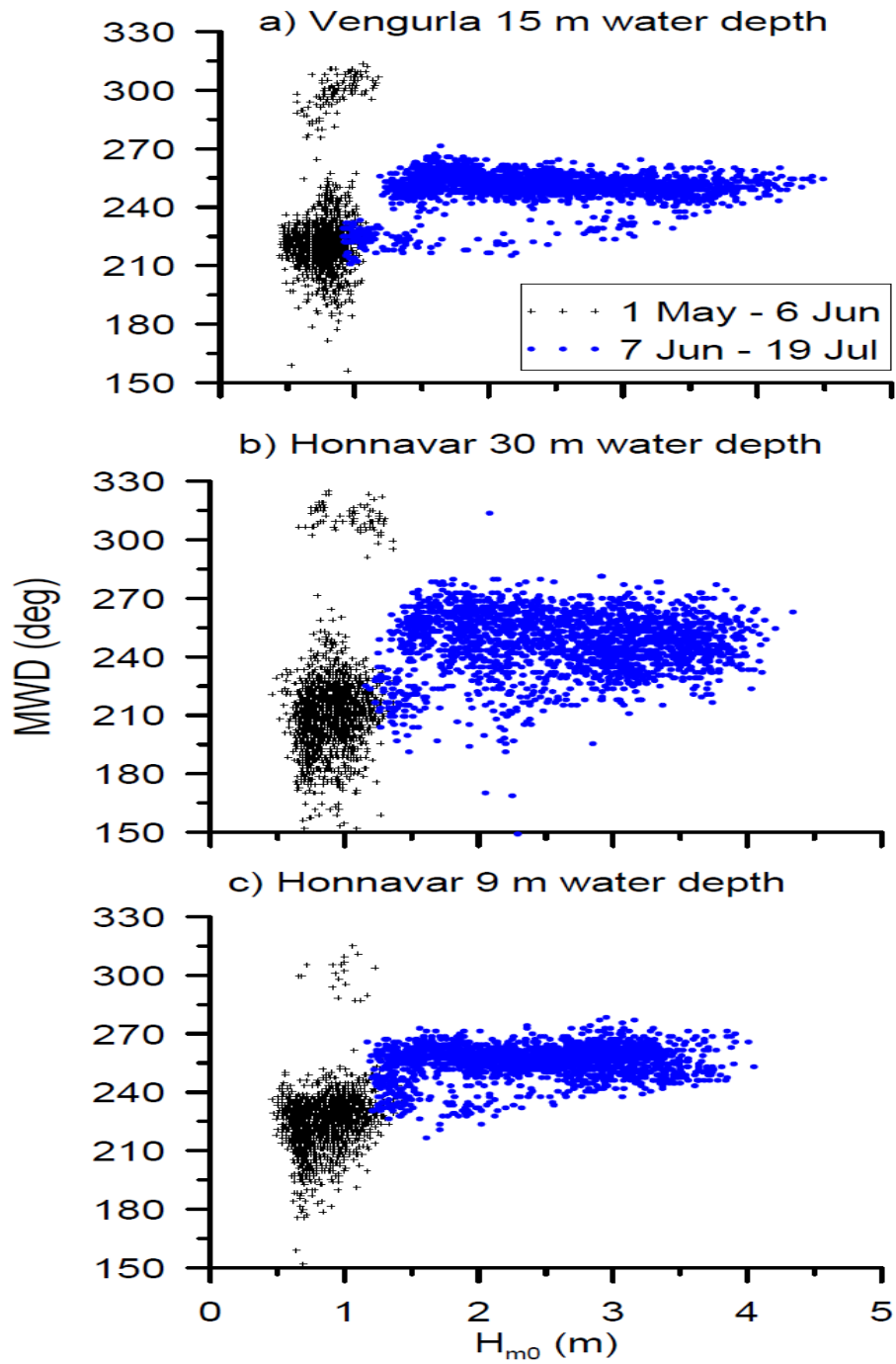


Figure 9. Joint distribution of significant wave height ( $H_{m0}$ ) and mean wave direction (MWD) from 1 May to 19 July 2014 a) off Vengurla at 15 m water depth, b) off Honnavar at 30 m water depth and c) off Honnavar at 9 m water depth

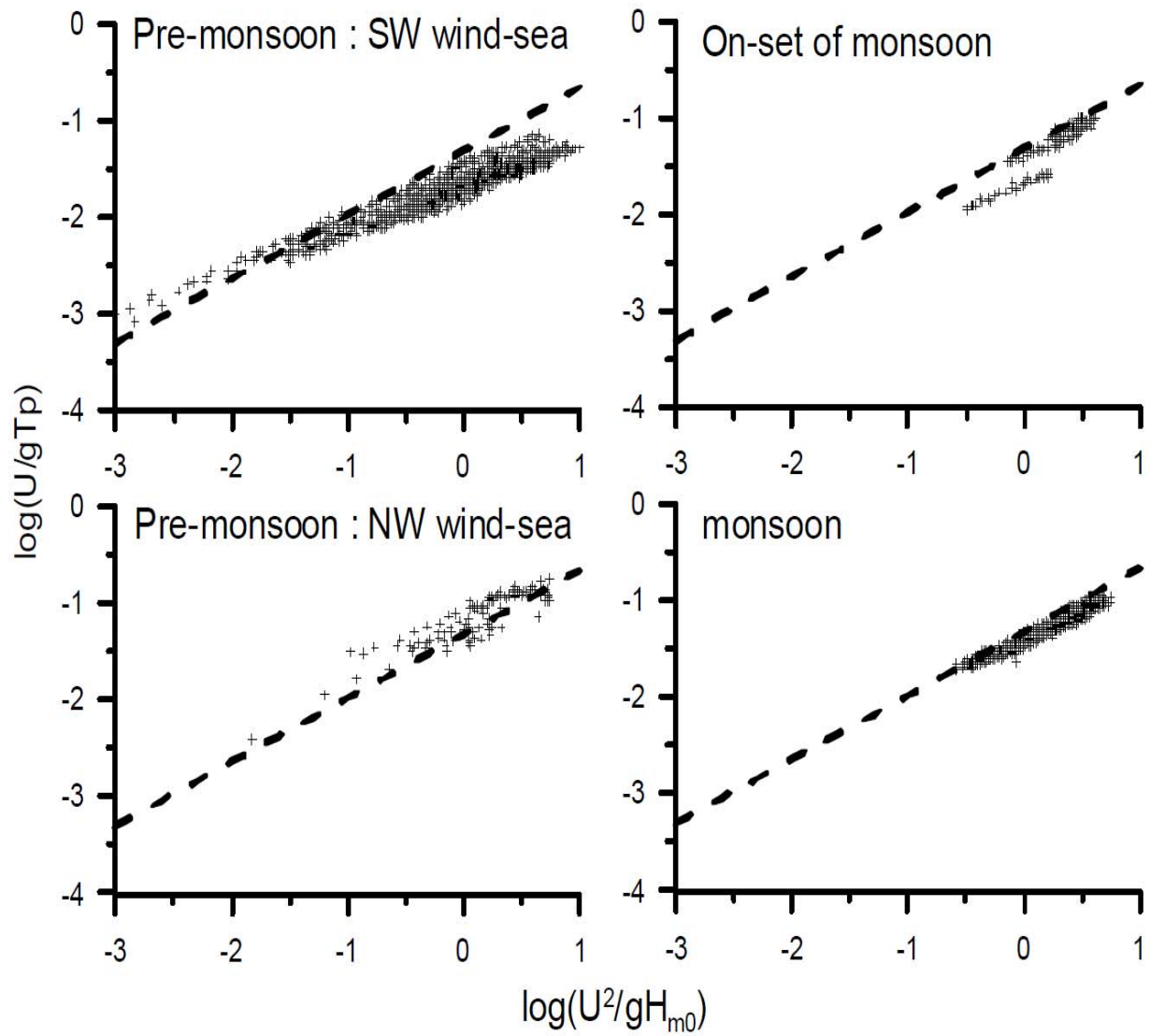


Figure 10. Plot of  $\log(U/gT_p)$  versus  $\log(U^2/gH_{m0})$  for wind-sea for the data measured before, during and after the onset of monsoon at Vengurla. Dashed line represents the theoretical relation given by Eq.1

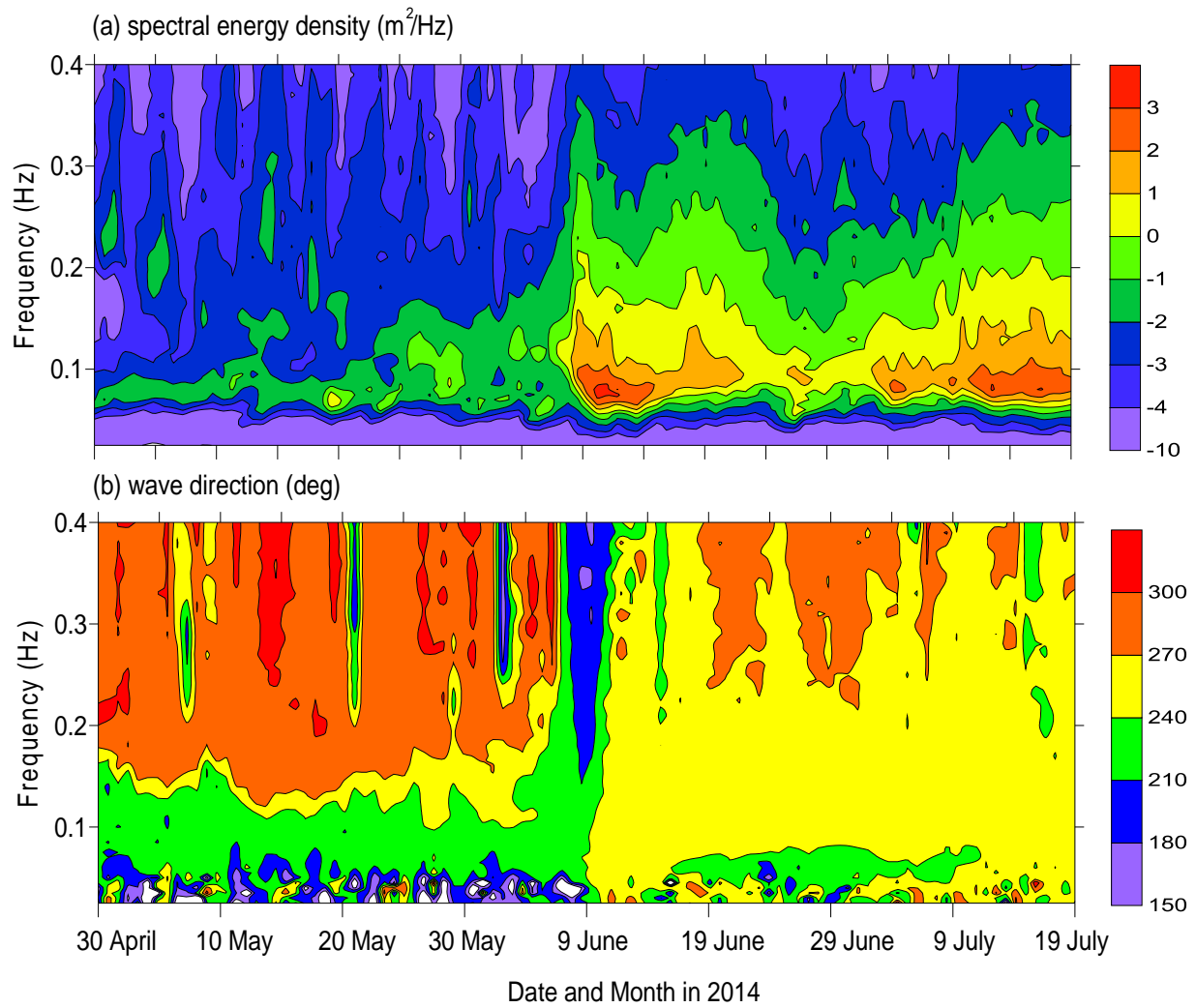


Figure 11. Contour plots of a) spectral energy density with frequency and b) mean wave direction with frequency from 1 May to 19 July 2014 off Vengurla

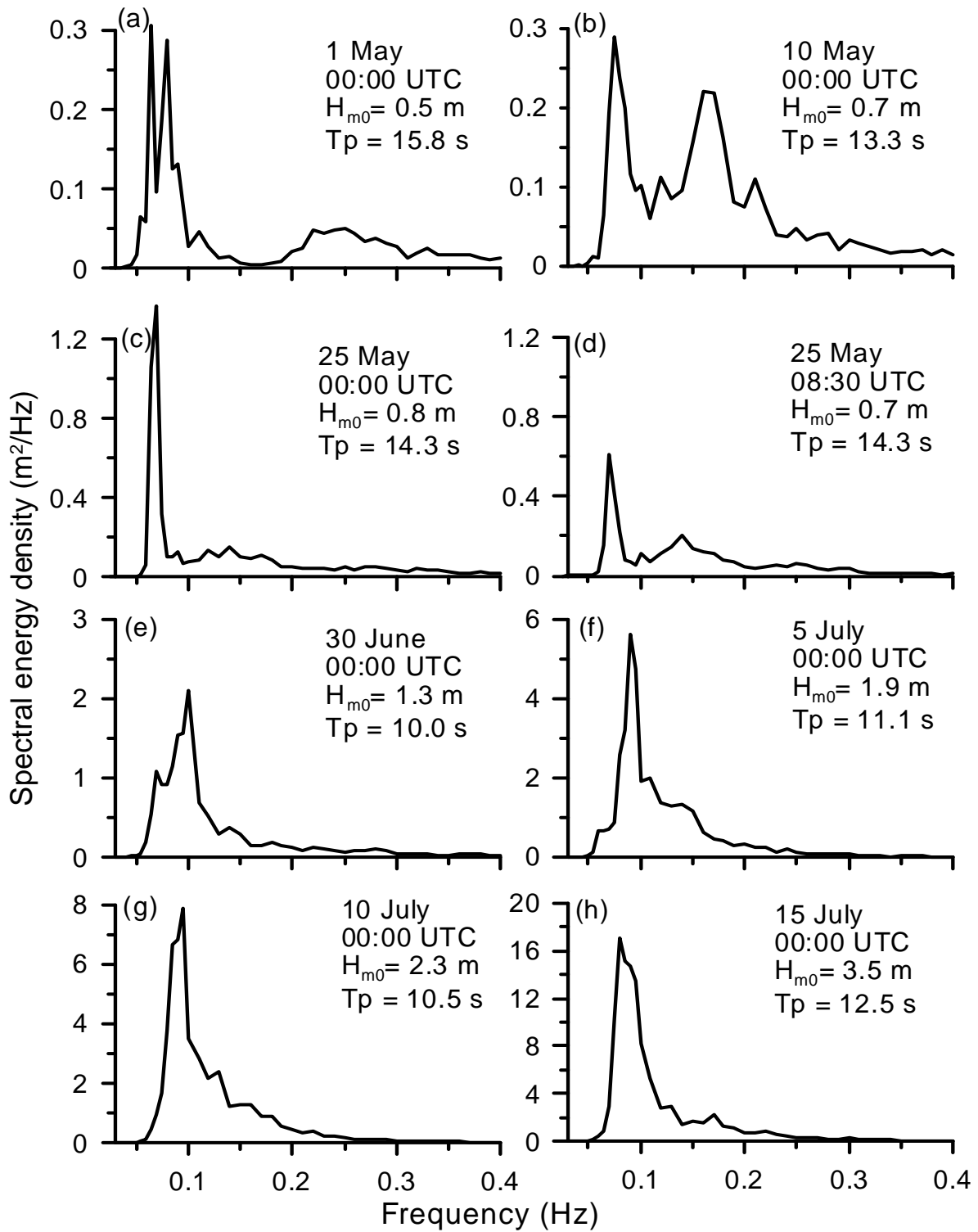


Figure 12. Typical single and multi peaked wave spectra during the study period off Vengurla



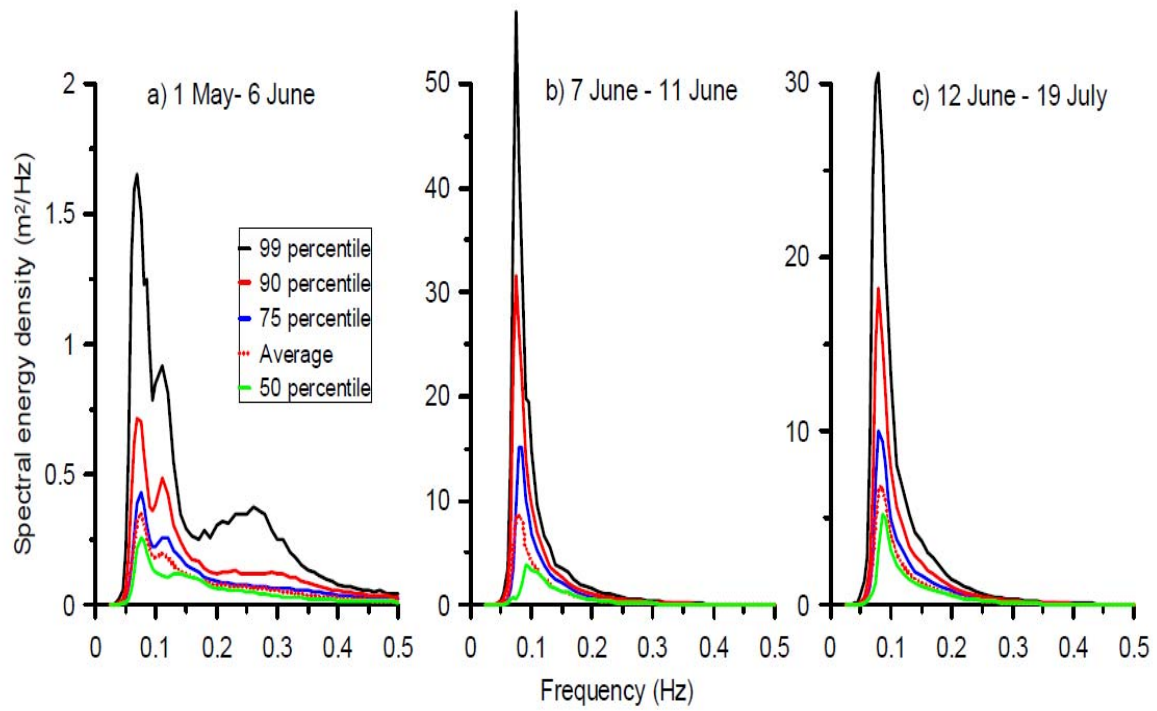


Figure 13. Averaged and the 99, 90, 75 and 50 percentile wave spectra during a) 1 May - 6 June, b) 7-11 June and c) 12 June-19 July off Vengurla

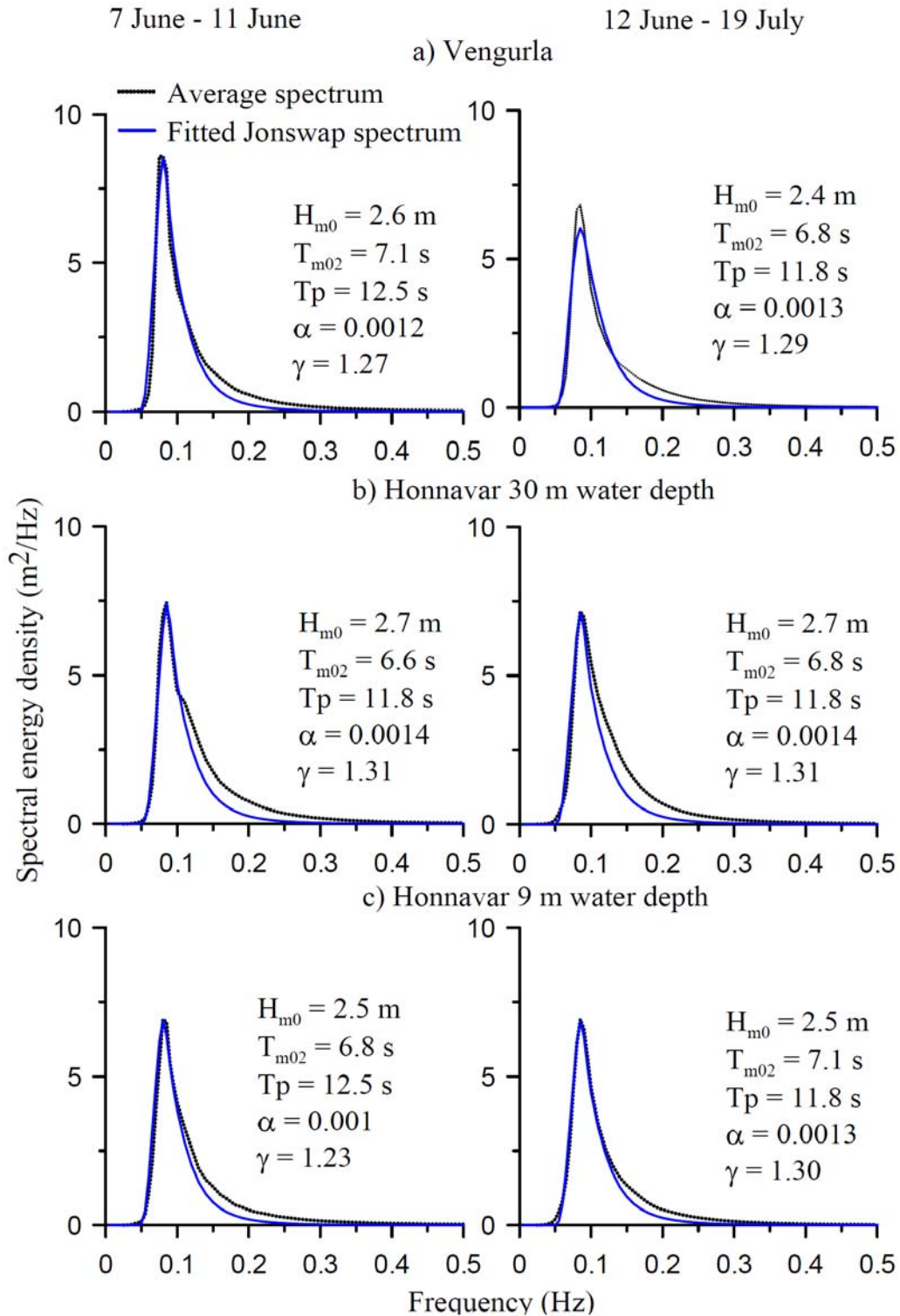


Figure 14. Average wave spectrum during onset of monsoon (left panel) and during monsoon (right panel) off Vengurla and off Honnavar. The fitted JONSWAP spectrum is also shown.